Metadata of the chapter that will be visualized in SpringerLink

Book Title	Supercomputing	
Series Title		
Chapter Title	The Simulation of 3D Wave Fields in Complex Topography Media	
Copyright Year	2019	
Copyright HolderName	Springer Nature Switzerland AG	
Corresponding Author	Family Name	**Titov**
	Particle	
	Given Name	**Pavel**
	Prefix	
	Suffix	
	Role	
	Division	
	Organization	Institute of Computational Mathematics and Mathematical Geophysics SB RAS
	Address	Novosibirsk, Russia
	Division	
	Organization	Trofimuk Institute of Petroleum Geology and Geophysics of SB RAS
	Address	Novosibirsk, Russia
	Email	tapawel@gmail.com

Abstract

A parallel algorithm for the simulation of wave field in 3D heterogeneous media with a curved free surface is proposed. In this paper we use a mapping method to transform the initial problem. It is based on the construction of a curvilinear mesh that conforms with the geometry of the free surface in the domain of interest. This domain is then to be mapped onto the “calculation” rectangular domain covered with a regular mesh. Therefore, now we have the initial problems restated in generalized coordinates but in the domain of simple geometry. To solve the transformed problem in the “calculation” domain, we use a finite difference method. Numerical tests were carried out on the SSCC cluster of SB RAS. The results of numerical simulation are presented.

Keywords: 3D - Wave field - Elasticity - Parallel algorithm - Simulation - Curvilinear mesh - Finite difference method

The Simulation of 3D Wave Fields in Complex Topography Media

Pavel Titov[1,2(✉)]

[1] Institute of Computational Mathematics and Mathematical Geophysics SB RAS, Novosibirsk, Russia
tapawel@gmail.com
[2] Trofimuk Institute of Petroleum Geology and Geophysics of SB RAS, Novosibirsk, Russia

Abstract. A parallel algorithm for the simulation of wave field in 3D heterogeneous media with a curved free surface is proposed. In this paper we use a mapping method to transform the initial problem. It is based on the construction of a curvilinear mesh that conforms with the geometry of the free surface in the domain of interest. This domain is then to be mapped onto the "calculation" rectangular domain covered with a regular mesh. Therefore, now we have the initial problems restated in generalized coordinates but in the domain of simple geometry. To solve the transformed problem in the "calculation" domain, we use a finite difference method. Numerical tests were carried out on the SSCC cluster of SB RAS. The results of numerical simulation are presented.

Keywords: 3D · Wave field · Elasticity · Parallel algorithm · Simulation · Curvilinear mesh · Finite difference method

1 Introduction

The numerical simulation of elastic waves is actively used in studying the seismic-wave propagation in 3D complex media. There are several principal methods to compute a wave field: Finite differences [1–5], finite elements [6], spectral elements [7,8], discontinuous Galerkin [9,10], finite volumes [11], and combinations of these methods [12–14]. Finite elements, discontinuous Galerkin and spectral methods can provide a high accuracy by increasing the dimension of the functional space used. The methods in question can be applied on irregular meshes. However the generation of a mesh in this case is time consuming and is difficult to automate. Finite difference methods are universal when solving such problems in the Cartesian coordinate system. These methods are applied in this paper. Note that often the domain under study can have a complex geometry of the free surface (solid/air interface). For the consistency of the numerical model and the physical model a curvilinear mesh is used. The theory of curvilinear meshes construction and application for solving real problems is considered in detail within [15–17]. As applied to the problems of elastodynamics, curvilinear meshes were

V. Voevodin and S. Sobolev (Eds.): RuSCDays 2019, CCIS 1129, pp. 1–12, 2019.
https://doi.org/10.1007/978-3-030-36592-9_37

utilized in [18,19] for a 2D case, and in [20–22] for 2D and 3D case, respectively. A distinctive feature of this paper is the use of the original mesh generator that allows better accuracy of numerical realization for the free surface conditions. From [20–22] author has taken a balance technique idea to construct the finite difference scheme. Considering the size of the domain in solving real-scale problems (tens of kilometers in each coordinate direction), it is necessary to carry out the numerical simulation using high-performance systems. The use of a curvilinear mesh in the finite difference method implies the original problem to be solved in generalized coordinates. The author has developed and implemented a parallel 3D algorithm using the Fortran language and the MPI library.

Both the test for the simulation of wave fields in heterogeneous medium as well as the test for the algorithm scalability, were carried out on the cluster NKS-30T of SSCC SB RAS.

2 Statement of the Problem

The wave field simulation is carried out based on the numerical solution of the elasticity linear system, expressed via displacements in Cartesian coordinates. If perturbations occur in a medium, the particles of the medium deviate from the equilibrium position when a wave passes through them. The deviation is represented by the displacement vector $(u, v, w)^T$. The density ρ, longitudinal waves speed V_p, share wave speed V_s and the Lame coefficients $\lambda = \rho(V_p^2 - 2V_s^2), \mu = \rho V_s^2$ are the medium parameters, $(F_x, F_y, F_z)^T$ is the mass force vector that represents a source of perturbations. Physical domain geometry is also considered to be given.

By restoring the displacement vector at each point of the domain at each time instant, we can simulate the process of elastic waves propogation.

The sequence of steps to solve the problem can be represented as follows:

1. Statement of the problem and its mathematical formulation in Cartesian and generalized coordinate systems.
2. Construction of a curvilinear mesh consistent with physical domain geometry.
3. Development of the numerical parallel algorithms to solve the problem.
4. Software implementation of the parallel numerical algorithms.
5. Conducting experiments on a parallel architecture for the complex media models.

2.1 Mathematical Model in Cartesian Coordinates

We introduce the following notations: $\partial\Gamma$ is the boundary of the domain inside the ground, ∂S is the free curvilinear surface. In Cartesian system (x, y, z), the equations are:

$$\begin{aligned}\rho\frac{\partial^2 u}{\partial t^2} &= \frac{\partial \sigma_{xx}}{\partial x} + \frac{\partial \sigma_{xy}}{\partial y} + \frac{\partial \sigma_{xz}}{\partial z} + F_x \\ \rho\frac{\partial^2 v}{\partial t^2} &= \frac{\partial \sigma_{xy}}{\partial x} + \frac{\partial \sigma_{yy}}{\partial y} + \frac{\partial \sigma_{yz}}{\partial z} + F_y \\ \rho\frac{\partial^2 w}{\partial t^2} &= \frac{\partial \sigma_{xz}}{\partial x} + \frac{\partial \sigma_{yz}}{\partial y} + \frac{\partial \sigma_{zz}}{\partial z} + F_z\end{aligned} \tag{1}$$

where
$\sigma_{xx} = (\lambda+2\mu)\frac{\partial u}{\partial x} + \lambda\frac{\partial v}{\partial y} + \lambda\frac{\partial w}{\partial z}$, $\sigma_{yy} = \lambda\frac{\partial u}{\partial x} + (\lambda+2\mu)\frac{\partial v}{\partial y} + \lambda\frac{\partial w}{\partial z}$,
$\sigma_{zz} = \lambda\frac{\partial u}{\partial x} + \lambda\frac{\partial v}{\partial y} + (\lambda+2\mu)\frac{\partial w}{\partial z}$, $\sigma_{xy} = \mu\frac{\partial u}{\partial y} + \mu\frac{\partial v}{\partial x}$, $\sigma_{xz} = \mu\frac{\partial u}{\partial z} + \mu\frac{\partial w}{\partial x}$,
$\sigma_{yz} = \mu\frac{\partial v}{\partial z} + \mu\frac{\partial w}{\partial y}$ are components of the stress tensor $\overline{\sigma}$.

Condition on the free surface ∂S: $\overline{\sigma}\cdot\overline{n} = 0$, or in the scalar form,

$$\begin{aligned}&n_x\left((\lambda+2\mu)\frac{\partial u}{\partial x} + \lambda\frac{\partial v}{\partial y} + \lambda\frac{\partial w}{\partial z}\right) + n_y\left(\mu\frac{\partial u}{\partial y} + \mu\frac{\partial v}{\partial x}\right) + n_z\left(\mu\frac{\partial u}{\partial z} + \mu\frac{\partial w}{\partial x}\right) = 0 \\ &n_x\left(\mu\frac{\partial u}{\partial y} + \mu\frac{\partial v}{\partial x}\right) + n_y\left(\lambda\frac{\partial u}{\partial x} + (\lambda+2\mu)\frac{\partial v}{\partial y} + \lambda\frac{\partial w}{\partial z}\right) + n_z\left(\mu\frac{\partial v}{\partial z} + \mu\frac{\partial w}{\partial y}\right) = 0 \\ &n_x\left(\mu\frac{\partial u}{\partial z} + \mu\frac{\partial w}{\partial y}\right) + n_y\left(\mu\frac{\partial v}{\partial z} + \mu\frac{\partial w}{\partial y}\right) + n_z\left(\lambda\frac{\partial u}{\partial x} + \lambda\frac{\partial v}{\partial y} + (\lambda+2\mu)\frac{\partial w}{\partial z}\right) = 0\end{aligned} \tag{2}$$

where $(n_x, n_y, n_z)^T$ is the unit normal to the free surface.

The conditions on the inside boundary $\partial\Gamma$ are:

$$u|_{\partial\Gamma} = v|_{\partial\Gamma} = w|_{\partial\Gamma} = 0 \tag{3}$$

The initial conditions:

$$u|_{t=0} = v|_{t=0} = w|_{t=0} = 0, \quad \left.\frac{\partial u}{\partial t}\right|_{t=0} = \left.\frac{\partial v}{\partial t}\right|_{t=0} = \left.\frac{\partial w}{\partial t}\right|_{t=0} = 0 \tag{4}$$

2.2 Mathematical Model in Generalized Coordinates

We consider (q^1, q^2, q^3) to be the new generalized coordinates. System (1) must be accordingly transformed:

$$\begin{aligned}\rho\frac{\partial^2 u}{\partial t^2} &= \frac{1}{J}\left(\frac{\partial \tilde{\sigma_1}}{\partial q^1} + \frac{\partial \tilde{\sigma_2}}{\partial q^2} + \frac{\partial \tilde{\sigma_3}}{\partial q^3}\right) + F_x \\ \rho\frac{\partial^2 v}{\partial t^2} &= \frac{1}{J}\left(\frac{\partial \tilde{\sigma_4}}{\partial q^1} + \frac{\partial \tilde{\sigma_5}}{\partial q^2} + \frac{\partial \tilde{\sigma_6}}{\partial q^3}\right) + F_y \\ \rho\frac{\partial^2 w}{\partial t^2} &= \frac{1}{J}\left(\frac{\partial \tilde{\sigma_7}}{\partial q^1} + \frac{\partial \tilde{\sigma_8}}{\partial q^2} + \frac{\partial \tilde{\sigma_9}}{\partial q^3}\right) + F_z\end{aligned} \tag{5}$$

where
$\tilde{\sigma_1} = J\left(\sigma_{xx}\frac{\partial q^1}{\partial x} + \sigma_{xy}\frac{\partial q^1}{\partial y} + \sigma_{xz}\frac{\partial q^1}{\partial z}\right)$, $\tilde{\sigma_2} = J\left(\sigma_{xx}\frac{\partial q^2}{\partial x} + \sigma_{xy}\frac{\partial q^2}{\partial y} + \sigma_{xz}\frac{\partial q^2}{\partial z}\right)$,

$$\tilde{\sigma_3} = J\left(\sigma_{xx}\frac{\partial q^3}{\partial x} + \sigma_{xy}\frac{\partial q^3}{\partial y} + \sigma_{xz}\frac{\partial q^3}{\partial z}\right),\ \tilde{\sigma_4} = J\left(\sigma_{xy}\frac{\partial q^1}{\partial x} + \sigma_{yy}\frac{\partial q^1}{\partial y} + \sigma_{yz}\frac{\partial q^1}{\partial z}\right),$$
$$\tilde{\sigma_5} = J\left(\sigma_{xy}\frac{\partial q^2}{\partial x} + \sigma_{yy}\frac{\partial q^2}{\partial y} + \sigma_{yz}\frac{\partial q^2}{\partial z}\right),\ \tilde{\sigma_6} = J\left(\sigma_{xy}\frac{\partial q^3}{\partial x} + \sigma_{yy}\frac{\partial q^3}{\partial y} + \sigma_{yz}\frac{\partial q^3}{\partial z}\right),$$
$$\tilde{\sigma_7} = J\left(\sigma_{xz}\frac{\partial q^1}{\partial x} + \sigma_{yz}\frac{\partial q^1}{\partial y} + \sigma_{zz}\frac{\partial q^1}{\partial z}\right),\ \tilde{\sigma_8} = J\left(\sigma_{xz}\frac{\partial q^2}{\partial x} + \sigma_{yz}\frac{\partial q^2}{\partial y} + \sigma_{zz}\frac{\partial q^2}{\partial z}\right),$$
$$\tilde{\sigma_9} = J\left(\sigma_{xz}\frac{\partial q^3}{\partial x} + \sigma_{yz}\frac{\partial q^3}{\partial y} + \sigma_{zz}\frac{\partial q^3}{\partial z}\right).$$

Components of the mass force vector are $F_x(t,\overline{x}) = F_x(t,x(\overline{q}),y(\overline{q}),z(\overline{q}))$, $F_y(t,\overline{x}) = F_y(t,x(\overline{q}),y(\overline{q}),z(\overline{q}))$, $F_z(t,\overline{x}) = F_z(t,x(\overline{q}),y(\overline{q}),z(\overline{q}))$

Here we offer only σ_{xx} in detail in order for reader to get a general idea of equations complexity and how it imposes additional difficulties for numerical solution: $\sigma_{xx} = (\lambda+2\mu)\sum_{i=1}^{3}\frac{\partial q^i}{\partial x}\frac{\partial u}{\partial q^i} + \lambda\sum_{i=1}^{3}\frac{\partial q^i}{\partial y}\frac{\partial v}{\partial q^i} + \lambda\sum_{i=1}^{3}\frac{\partial q^i}{\partial z}\frac{\partial w}{\partial q^i}$.

The rest components of the stress tensor $\overline{\sigma}$ are to be transformed the same way. And as for the free surface condition (2), it transforms into:

$$\begin{gathered}
n_x\left((\lambda+2\mu)\sum_{i=1}^{3}\frac{\partial q^i}{\partial x}\frac{\partial u}{\partial q^i} + \lambda\sum_{i=1}^{3}\frac{\partial q^i}{\partial y}\frac{\partial v}{\partial q^i} + \lambda\sum_{i=1}^{3}\frac{\partial q^i}{\partial z}\frac{\partial w}{\partial q^i}\right) + \\
n_y\left(\mu\sum_{i=1}^{3}\frac{\partial q^i}{\partial y}\frac{\partial u}{\partial q^i} + \mu\sum_{i=1}^{3}\frac{\partial q^i}{\partial x}\frac{\partial v}{\partial q^i}\right) + n_z\left(\mu\sum_{i=1}^{3}\frac{\partial q^i}{\partial z}\frac{\partial u}{\partial q^i} + \mu\sum_{i=1}^{3}\frac{\partial q^i}{\partial x}\frac{\partial w}{\partial q^i}\right) = 0 \\
n_x\left(\mu\sum_{i=1}^{3}\frac{\partial q^i}{\partial y}\frac{\partial u}{\partial q^i} + \mu\sum_{i=1}^{3}\frac{\partial q^i}{\partial x}\frac{\partial v}{\partial q^i}\right) + \\
n_y\left(\lambda\sum_{i=1}^{3}\frac{\partial q^i}{\partial x}\frac{\partial u}{\partial q^i} + (\lambda+2\mu)\sum_{i=1}^{3}\frac{\partial q^i}{\partial y}\frac{\partial v}{\partial q^i} + \lambda\sum_{i=1}^{3}\frac{\partial q^i}{\partial z}\frac{\partial w}{\partial q^i}\right) + \\
n_z\left(\mu\sum_{i=1}^{3}\frac{\partial q^i}{\partial z}\frac{\partial v}{\partial q^i} + \mu\sum_{i=1}^{3}\frac{\partial q^i}{\partial y}\frac{\partial w}{\partial q^i}\right) = 0 \\
n_x\left(\mu\sum_{i=1}^{3}\frac{\partial q^i}{\partial z}\frac{\partial u}{\partial q^i} + \mu\sum_{i=1}^{3}\frac{\partial q^i}{\partial x}\frac{\partial w}{\partial q^i}\right) + n_y\left(\mu\sum_{i=1}^{3}\frac{\partial q^i}{\partial z}\frac{\partial v}{\partial q^i} + \mu\sum_{i=1}^{3}\frac{\partial q^i}{\partial y}\frac{\partial w}{\partial q^i}\right) + \\
n_z\left(\lambda\sum_{i=1}^{3}\frac{\partial q^i}{\partial x}\frac{\partial u}{\partial q^i} + \lambda\sum_{i=1}^{3}\frac{\partial q^i}{\partial y}\frac{\partial v}{\partial q^i} + (\lambda+2\mu)\sum_{i=1}^{3}\frac{\partial q^i}{\partial z}\frac{\partial w}{\partial q^i}\right) = 0
\end{gathered} \tag{6}$$

where $(x^1,x^2,x^3) = (x,y,z)$, $J = det\left(\frac{\partial x^i}{q^j}\right)$, and $\frac{\partial q^i}{\partial x^j} = \frac{1}{J}\left(\frac{\partial x^{j+1}}{\partial q^{i+1}}\frac{\partial x^{j+2}}{\partial q^{i+2}} - \frac{\partial x^{j+1}}{\partial q^{i+2}}\frac{\partial x^{j+2}}{\partial q^{i+1}}\right)$ with the cyclic numeration $i,j = 1,2,3$. Components $\frac{\partial q^i}{\partial x^j}$ are a metrical coefficients. They are defined by properties of the curvilinear mesh. The normal unit vector in generalized coordinates is

$$(n_x, n_y, n_z) = \frac{\left(\frac{D(y,z)}{D(q^1,q^2)}, \frac{D(z,x)}{D(q^1,q^2)}, \frac{D(x,y)}{D(q^1,q^2)}\right)}{\sqrt{\left(\frac{D(x,y)}{D(q^1,q^2)}\right)^2 + \left(\frac{D(y,z)}{D(q^1,q^2)}\right)^2 + \left(\frac{D(z,x)}{D(q^1,q^2)}\right)^2}}$$

with $\frac{D(x,y)}{D(q^1,q^2)} = \frac{\partial x}{\partial q^1}\frac{\partial y}{\partial q^2} - \frac{\partial x}{\partial q^2}\frac{\partial y}{\partial q^1}$, $\frac{D(y,z)}{D(q^1,q^2)} = \frac{\partial y}{\partial q^1}\frac{\partial z}{\partial q^2} - \frac{\partial y}{\partial q^2}\frac{\partial z}{\partial q^1}$, $\frac{D(z,x)}{D(q^1,q^2)} = \frac{\partial z}{\partial q^1}\frac{\partial x}{\partial q^2} - \frac{\partial z}{\partial q^2}\frac{\partial x}{\partial q^1}$.

Boundary conditions (3) and initial conditions (4) remain the same.

Now the equations in generalized coordinates are to be solved within a domain of simple parallelepiped shape, that can be covered with regular 3D mesh.

3 Constructing a Curvilinear Mesh

The technique of constructing a 3D mesh is considered in [12]. The main advantage of building a mesh with the method described, is that the mesh nodes are calculated analytically which means good scalability potential for the numerical realization. In this study we will just note an important point: near the free surface, all the coordinate lines of a curvilinear mesh are mutually orthogonal. This way we can obtain better approximation accuracy of the free surface condition.

Also, we should mention, that due to specific features of the finite difference approximation of equations (5), (6), every cell unit for each discrete node of the displacement vector $(u, v, w)^T$ consists of eight cell units of a curvilinear mesh (Fig. 1). It allows better accuracy of metric coefficients and Jacobian approximation.

4 Finite Difference Approximation

According to the results obtained in [12], the finite difference method possesses a good scalability potential.

The factors ρ, λ, μ and u, v, w are positioned at the center of the cell unit. The metrical coefficients and Jacobian are positioned at the center as well as in the middle of every edge and side of the cell unit (Fig. 1). The indices (i, j, k) are consistent with the axes (Oq^1, Oq^2, Oq^3).

The position of u, v, w is explained by the complexity of equations (5). Unlike as it is in [3], there is no benefit of using a staggered mesh. It would widen the scheme template and, therefore, make worse the accuracy.

In order to develop a finite difference scheme, we have applied a balance technique to (5). It is considered in detail in [23] for the case of Cartesian coordinates.

V is the unit cell volume in Cartesian coordinates, V' is the corresponding unit cell volume in generalized coordinates, which in our case has a cubic shape. The length of V' edges in each direction is considered to be $h_{q^1} = h_{q^2} = h_{q^3} = h$,

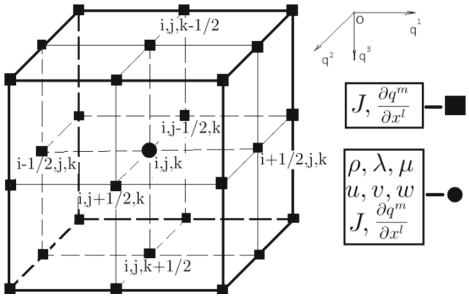

Fig. 1. A scheme of elements position in cell units

S' is the boundary of V'. Also, $S' = \sum_{m=1}^{6} S'_m$, where S'_1 is the side that contains the node $(i-1/2, j, k)$, and S'_2 - $(i+1/2, j, k)$, S'_3 - $(i, j-1/2, k)$, S'_4 - $(i, j+1/2, k)$, S'_5 - $(i, j, k-1/2)$, S'_6 - $(i, j, k+1/2)$, respectively. Here we will only illustrate as an example how the balance technique is applied to the first equation of (1) and (5). Integrating over a unit cell volume V

$$\int_V \rho \frac{\partial^2 u}{\partial t^2} dV = \int_V \left(\frac{\partial \sigma_{xx}}{\partial x} + \frac{\partial \sigma_{xy}}{\partial y} + \frac{\partial \sigma_{xz}}{\partial z} \right) dV + \int_V F_x dV \tag{7}$$

and using the substitution of variables in (7) we come to:

$$\int_{V'} J\rho \frac{\partial^2 u}{\partial t^2} dV' = \int_{V'} \left(\frac{\partial \tilde{\sigma_1}}{\partial q^1} + \frac{\partial \tilde{\sigma_2}}{\partial q^2} + \frac{\partial \tilde{\sigma_3}}{\partial q^3} \right) dV' + \int_{V'} JF_x dV' \tag{8}$$

Applying the divergence theorem to (8) we have the following:

$$\int_{V'} J\rho \frac{\partial^2 u}{\partial t^2} dV' = \oint_{S'} \left(\tilde{\sigma_1} n_1 + \tilde{\sigma_2} n_2 + \tilde{\sigma_3} n_3 \right) dS' + \int_{V'} JF_x dV' \tag{9}$$

where (n_1, n_2, n_3) is a unit normal to $\partial S'$. Then (9) can be rewritten as:

$$\begin{aligned} \int_{V'} J\rho \frac{\partial^2 u}{\partial t^2} dV' = &- \oint_{S'_1} \tilde{\sigma_1} dS' + \oint_{S'_2} \tilde{\sigma_1} dS' - \oint_{S'_3} \tilde{\sigma_2} dS' + \oint_{S'_4} \tilde{\sigma_2} dS' - \\ &\oint_{S'_5} \tilde{\sigma_3} dS' + \oint_{S'_6} \tilde{\sigma_3} dS' + \int_{V'} JF_x dV' \end{aligned} \tag{10}$$

For the convenience we will define finite-difference operators that are used for constructing the scheme. Here h is the discrete space step, τ is the discrete time step. $A^N_{i,j,k} = A(N\tau, ih, jh, kh)$, and for Jacobian and metrical coefficients $B_{i,j,k} = B(ih/2, jh/2, kh/2)$.

$$D_{tt}[f]^N_{i,j,k} = \frac{1}{\tau^2} \left(f^{N+1}_{i,j,k} - 2f^N_{i,j,k} + f^{N-1}_{i,j,k} \right) = \frac{\partial^2 f}{\partial t^2}(N\tau, ih, jh, kh) + O(\tau^2),$$

$$D_1[f]^N_{i-1/2,j,k} = \frac{1}{h}\left(f^N_{i,j,k} - f^N_{i-1,j,k}\right) = \frac{\partial f}{\partial q^1}(N\tau, ih - h/2, jh, kh) + O(q^1 q^1),$$
$$D_2[f]^N_{i,j-1/2,k} = \frac{1}{h}\left(f^N_{i,j,k} - f^N_{i,j-1,k}\right) = \frac{\partial f}{\partial q^2}(N\tau, ih, jh - h/2, kh) + O(q^2 q^2),$$
$$D_3[f]^N_{i,j,k-1/2} = \frac{1}{h}\left(f^N_{i,j,k} - f^N_{i,j,k-1}\right) = \frac{\partial f}{\partial q^3}(N\tau, ih, jh, kh - h/2) + O(q^3 q^3),$$

And

$$D_1[f]^N_{i,j-1/2,k} = \frac{1}{4}\Big(D_1[f]^N_{i-1/2,j,k} + D_1[f]^N_{i+1/2,j,k} + D_1[f]^N_{i-1/2,j-1,k} + D_1[f]^N_{i+1/2,j-1,k}\Big),$$

$$D_1[f]^N_{i,j,k-1/2} = \frac{1}{4}\Big(D_1[f]^N_{i-1/2,j,k} + D_1[f]^N_{i+1/2,j,k} + D_1[f]^N_{i-1/2,j,k-1} + D_1[f]^N_{i+1/2,j,k-1}\Big).$$

The rest operators $D_2[f]^N_{i-1/2,j,k}, D_2[f]^N_{i,j,k-1/2}, D_3[f]^N_{i-1/2,j,k}, D_2[f]^N_{i,j-1/2,k}$ are being defined in the same manner. Now the scheme for (10) in terms of the above-described operators with allowance for the mean value theorem, takes the form

$$\rho_{i,j,k} J_{2i,2j,2k} D_{tt}[u]^N_{i,j,k} = \frac{1}{h}\Big(-\tilde{\sigma_1}^N_{i-1/2,j,k} + \tilde{\sigma_1}^N_{i+1/2,j,k} - \tilde{\sigma_2}^N_{i,j-1/2,k} + \tilde{\sigma_2}^N_{i,j+1/2,k} - \tilde{\sigma_3}^N_{i,j,k-1/2} + \tilde{\sigma_3}^N_{i,j,k+1/2}\Big) + J_{2i,2j,2k} F^N_{i,j,k} \tag{11}$$

The detailed scheme for the first component of the right-hand side in (11) is as follows:

$$\tilde{\sigma_1}^N_{i-1/2,j,k} = J_{2i-1,2j,2k}\left(\sigma_{xx}{}^N_{i-1/2,j,k}\left(\frac{\partial q^1}{\partial x}\right)_{2i-1,2j,2k} + \sigma_{xy}{}^N_{i-1/2,j,k}\left(\frac{\partial q^1}{\partial y}\right)_{2i-1,2j,2k} + \sigma_{xz}{}^N_{i-1/2,j,k}\left(\frac{\partial q^1}{\partial z}\right)_{2i-1,2j,2k}\right) \tag{12}$$

The rest components of (11) are to be done in the same manner. And, finally, for $\sigma_{xy}{}^N_{i-1/2,j,k}$ in (12) the finite difference scheme is:

$$\sigma_{xy}{}^N_{i-1/2,j,k} = \frac{1}{2}(\mu_{i-1,j,k} + \mu_{i,j,k}) \sum_{m=1}^{3}\left(\frac{\partial q^m}{\partial y}\right)_{2i-1,2j,2k} D_m[u]^N_{i-1/2,j,k} + \frac{1}{2}(\mu_{i-1,j,k} + \mu_{i,j,k}) \sum_{m=1}^{3}\left(\frac{\partial q^m}{\partial x}\right)_{2i-1,2j,2k} D_m[v]^N_{i-1/2,j,k}$$

where

$$\left(\frac{\partial q^m}{\partial x^l}\right)_{2i-1,2j,2k} = \frac{1}{J_{2i-1,2j,2k}}\left(D_{m+1}[x^{l+1}]_{2i-1,2j,2k} D_{m+2}[x^{l+2}]_{2i-1,2j,2k} - D_{m+2}[x^{l+1}]_{2i-1,2j,2k} D_{m+1}[x^{l+2}]_{2i-1,2j,2k}\right).$$

The rest components of the stress tensor $\overline{\sigma}$ are to be approximated the same way. For the free surface condition, approximation does not differ from the one covered in [12]. Overall, the scheme proposed provides second accuracy order with respect to space and time, except for the interfaces between two layers with different media parameters. In this case, accuracy reduces to first order in space and to second order in time.

5 Parallel Algorithm and Its Realization

In this section we use the same technology as in [12]. In general, we decompose the domain to small 3D-cubes, every one of which is being assigned to a single process to realize the above finite difference scheme. After every time step, the neighboring processes conduct the data exchange via created 3D-cube topology. Each process has 26 neighbors. The parallel program was developed by means of the Fortran language and the MPI library.

6 Numerical Simulation and Scalability Tests

Numerical tests are carried out on the NKS-30T cluster of SSCC SB RAS, on SL390S G7 servers, each having 2×6 core Xeon X5670 2.93 GHz and 96 Gb RAM). In our case we have used CPUs exclusively.

For the simulation tests we have chosen the domain shown in Fig. 2, with corresponding mesh in Fig. 3. The medium parameters are: size $18.0 \times 18.0 \times 12.0$ km; for layers I and III: $\rho = 1.0\,\mathrm{g/cm^3}$, $V_p = 1.0\,\mathrm{km/s}$, $V_p = 0.5\,\mathrm{km/s}$; for layer II: $\rho = 0.81\,\mathrm{g/cm^3}$, $V_p = 0.888\,\mathrm{km/s}$, $V_s = 0.222\,\mathrm{km/s}$. The wave generator is of a "pressure center" type, located at $(x_0, y_0, z_0) = (5.5\,\mathrm{km},\ 9.0\,\mathrm{km},\ 0.5\,\mathrm{km})$. For elements of $F = (F_x, F_y, F_z)$ we consider

$$F_x = \begin{cases} \dfrac{\partial \delta(x - x_0, y - y_0, z - z_0)}{\partial x} F_1(t), & 0 \le t \le 2, \\ 0, & t > 2, \end{cases}$$

$$F_y = \begin{cases} \dfrac{\partial \delta(x - x_0, y - y_0, z - z_0)}{\partial y} F_1(t), & 0 \le t \le 2, \\ 0, & t > 2, \end{cases}$$

$$F_z = \begin{cases} \dfrac{\partial \delta(x - x_0, y - y_0, z - z_0)}{\partial z} F_1(t), & 0 \le t \le 2, \\ 0, & t > 2, \end{cases}$$

where $F_1(t) = sin(\pi t - \pi) + 0.8sin(2\pi t - 2\pi) + 0.2sin(3\pi t - 3\pi)$ and $\delta(x, y, z)$ is the Dirac delta.

The discrete domain size is $900 \times 900 \times 600$ points, and the size of the curvilinear mesh is $1801 \times 1801 \times 1201$ points. The required amount of RAM for such a size of a problem is around 290 GB. In Fig. 4, the results of the wave field

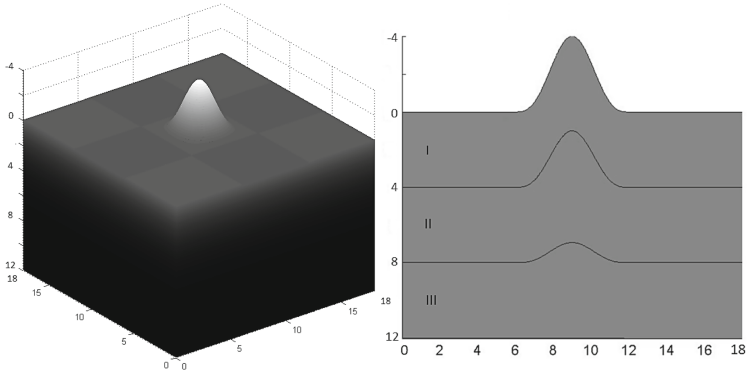

Fig. 2. The domain and its vertical slice with heterogeneous layers

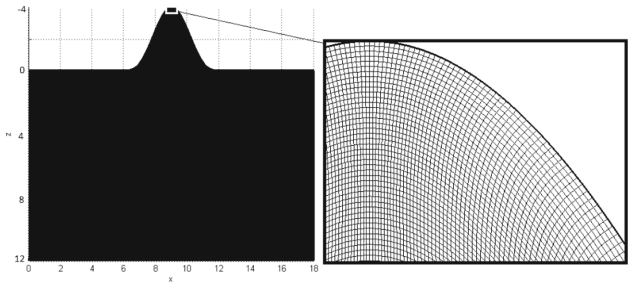

Fig. 3. Curvilinear mesh

simulation for the component W of the displacement vector are presented. The snapshots are taken from the cross-section that is parallel to the plane OXZ and contains the point of the source position (x_0, y_0, z_0). Also, in the Courant stability condition $V_p\tau/h \leq C/\sqrt{3}$, we have taken $C = 0.34$.

To study the strong scalability properties of the parallel program and algorithm developed, to each SL390S G7 server that has 12 cores, the cube with the size of $240 \times 240 \times 240$ points was assigned. The shape of the free surface or medium parameters do not matter for such a test. We proportionally increase the size of the domain and the number of cores. Thus, the amount of computation for each server remains the same, but the total number of data exchanges between processes increases. Each core conducts one thread of calculations. Ideally, the program execution time must not change, in which case the efficiency is considered to be unity. However the presence of data exchanges impacts the efficiency. Figure 5 shows the test results from which it can be seen that the algorithm and the program have good scalability properties. Within the range from 12 to 72 cores the efficiency drops to 0,946 and remains consistent through the increase from 72 to 120 cores.

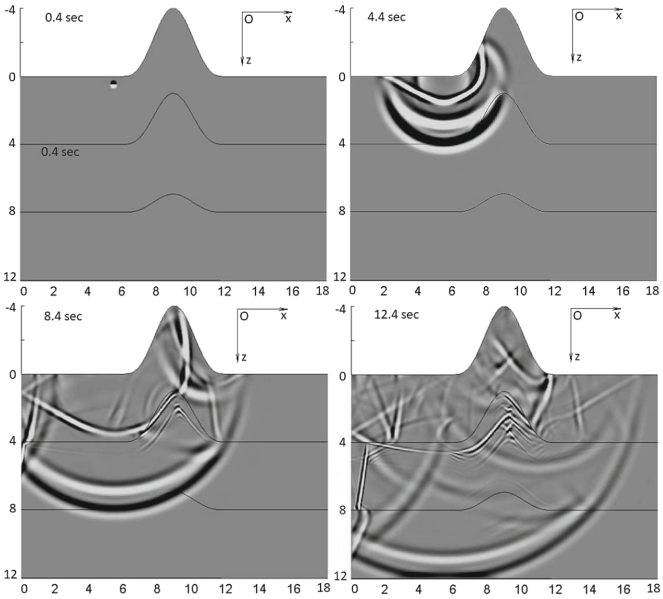

Fig. 4. Wave field at the time instants 0.4 s, 4.4 s, 8.4 s, 12.4 s

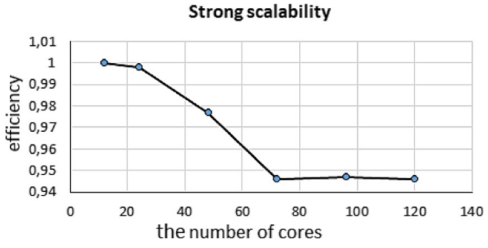

number of cores	efficiency
120	0,946
96	0,947
72	0,946
48	0,977
24	0,998
12	1

Fig. 5. The results of the strong scalability tests

7 Conclusion

This paper proposes the algorithm of 3D seismic waves simulation in elastic heterogeneous media for the domain with complex free surface geometry. The problem is formulated in terms of displacements in Cartesian and in generalized coordinates. Constructing a curvilinear mesh allows good consistency between physical domain and computational domain. The main result of this paper is the creation of the parallel 3D algorithm and its software implementations aimed at the numerical modeling of elastic waves in isotropic heterogeneous 3D media with complex free surface geometry. The algorithm was developed using the balance technique and finite difference method. The novelty of the scheme constructed is the positioning of metrical coefficients with respect to components of the displacement vector, which allows better accuracy. The algorithm developed shows

good results in terms of strong scalability. Further, the algorithm improvement we see as: utilizing the CCPML method [24] to dispose of the side boundary reflections; to adapt the program for other architectures like Intel Xeon Phi; to increase the scalability and the energy efficiency of the algorithm by optimizing RAM usage and data exchange.

Acknowledgement. The theoretical part of this research (Sects. 1, 2) has been supported by the Russian Science Foundation, project 17-17-01128. Work on Sects. 3, 4 was conducted within the framework of the budget project 0315-2019-0009 for ICMMG SB RAS, and for the technical part, Sects. 5 and 6, were supported by the RFBR grants 19-07-00085 and 18-07-00757 respectively.

All simulations have been done using the equipment of the Siberian Supercomputer Center.

References

1. Lebedev, V.I.: Difference analogues of orthogonal decompositions of basic differential operators and some boundary value problems. Comput. Math. Math. Phys. **4**, 449–465 (1964)
2. Alford, R.M., Kelly, K.R., Boore, D.M.: Accuracy of finite-difference modeling of the acoustic wave equation. Geophysics **39**, 834–842 (1974)
3. Virieux, J.: P-SV wave propagation in heterogeneous media: velocitystress finite-difference method. Geophysics **51**, 889–901 (1986)
4. Levander, A.R.: Fourth-order finite-difference P-SV seismograms. Geophysics **53**, 1425–1436 (1988)
5. Saenger, E.H., Gold, N., Shapiro, S.A.: Modeling the propagation of the elastic waves using a modified finite-difference grid. Wave Motion **31**, 77–92 (2000)
6. Zhang, J., Verschuur, D.J.: Elastic wave propagation in heterogeneous anisotropic media using the lumped finite-element method. Geophysics **67**, 625–638 (2002)
7. Komatitsch, D., Vilotte, J.-P.: The spectral element method: an efficient tool to simulate the seismic response of 2D and 3D geological structures. Bull. Seismol. Soc. Am. **88**, 368–392 (1998)
8. Tromp, J., Komatitsch, D., Liu, Q.: Spectral-element and adjoint methods in seismology. Commun. Comput. Phys. **3**, 1–32 (2008)
9. Grote, M.J., Schneebeli, A., Schotzau, D.: Discontinuous Galerkin finite element method for the wave equation. SIAM J. Numer. Anal. **44**, 2408–2431 (2006)
10. Etienne, V., Chaljub, E., Virieux, J., Glinsky, N.: An *hp*-adaptive discontinuous Galerkin finite-element method for 3D elastic wave modelling. Geophys. J. Int. **183**, 941–962 (2010)
11. Zhang, J.: Quadrangle-grid velocity-stress finite-difference method for elastic-wave-propagation simulation. Geophys. J. Int. **131**, 127–134 (1997)
12. Dumbser, M., Kaser, M.: An arbitrary high-order discontinuous Galerkin method for elastic waves on unstructured meshes II. Three-dimensional isotropic case. Geophys. J. Int. **167**, 319–336 (2006)
13. Kaser, M., Dumbser, M.: An arbitrary high-order discontinuous Galerkin method for elastic waves on unstructured meshes - I. The two-dimensional isotropic case with external source terms. Geophys. J. Int. **166**, 855–877 (2006)

14. Zhang, L., Wei, L., Lixin, H., Xiaogang, D., Hanxin, Z.: A class of hybrid DG/FV methods for conservation laws II: two-dimensional cases. J. Comput. Phys. **231**, 1104–1120 (2012)
15. Liseykin, V.: Difference Meshes. Theory and Applications, p. 254. SB RAS Publishing, Novosibirsk (2014). (in Russian)
16. Khakimzyanov G., Shokin Yu.: Difference schemes on adaptive meshes. Editorial and Publishing Center of NSU SB RAS, 130 p. (2005). (in Russian)
17. Yu, S., Danaev, N., Khakimzyanov, G., Shokina, N.: Lectures on difference schemes on moving meshes. Editorial and Publishing Center of KazNU Named After Al-Farabi, 183 p. (2005). (in Russian)
18. Daniel Appelo, N., Petersson, N.A.: A stable finite difference method for the elastic wave equation on complex geometries with free surfaces. Commun. Comput. Phys. **5**(1), 84–107 (2009)
19. Jose, M., Carcione, J.M.: The wave equation in generalized coordinates. Geophysics **59**(12), 1911–1919 (1994)
20. Titov, P.: An algorithm and a program for simulation of 2D-wave fields in areas with a curved free surface. In: Materials of the Conference "Scientific Service on the Internet - 2014" Novorossiysk, Abrau-Dyurso, 21–26 September 2014, pp. 446–455. (in Russian)
21. Titov, P.: Modeling of elastic waves in media with a complex free surface topography. Vestnik of NSU: Inf. Technol. **164**, 153–166 (2018). (in Russian)
22. Titov, P.: A technology of modeling of elastic waves propagation in media with complex 3D geometry of the surface with the aid of high performance cluster. In: Proceedings of Russian Supercomputing Days, pp. 1020–1031 (2016)
23. Vishnevsky, D., Lisitsa, V., Tcheverda, V., Reshetova, G.: Numerical study of the interface errors of finite-difference simulations of seismic waves. Geophysics **79**(4), T219–T232 (2014)
24. Komatitsch, D., Martin, R.: An unsplit convolutional perfectly matched layer improved at grazing incidence for the seismic wave equation. Geophysics **72**(5), SM155–SM167 (2007)